energy&fuels

pubs.acs.org/EF Article

# Study of Asphaltene Deposition onto Stainless-Steel Surfaces Using Quartz Crystal Microbalance with Dissipation

Fang Liu,* Scott Hickman, Tabish Maqbool, Vincent Pauchard, and Sanjoy Banerjee

Cite This: https://dx.doi.org/10.1021/acs.energyfuels.0c00663 Read Online

ACCESS | Metrics & More | Article Recommendations

**ABSTRACT:** Asphaltene deposition is one of the major flow assurance problems in upstream and downstream crude oil recovery operations. In order to prevent potential loss and reduce downtime due to asphaltenes, it is critical to understand the physics of asphaltene adsorption. This study presents a preliminary investigation of asphaltene adsorption from crude oils onto stainless-steel surfaces using the quartz crystal microbalance with dissipation (QCM-D) technique and proposes a theoretical interpretation of the deposition mechanism for asphaltene molecules. The kinetics of deposition at different concentrations was examined, and the sizes of the deposited asphaltene molecules were estimated from the initial adsorption kinetics. Numerical analysis of the experimental data using the theoretical two-step deposition model was attempted, and the optimized adsorption parameters proved to be quite close to those values obtained for some rock types in earlier adsorption studies. Despite asphaltene precipitation increasing with increasing heptane percentage, the deposition of asphaltenes was found to be maximum at 70 vol% heptane content. The performance of a commercial inhibitor was then assessed under different conditions using the developed experimental metrics, and the inhibitor was found to be able to reduce the maximum deposition amount at the solubility with 70 vol% heptane fraction, which happens to be the same condition that generates the largest amount of deposition. The information gained on the solubility effect and inhibitor performance is essential to help the industry better manage asphaltene-related flow assurance problems in crude oil recovery.

## 1. INTRODUCTION

In crude oil recovery processes, asphaltene deposits are often observed, and this can happen at different stages of production. Due to changes in temperature, pressure, chemical composition of crude oil, type of surface materials, composition of processing fluids, duration of contact among different phases, shear rate, and aging period,[1,2] asphaltenes can precipitate from crude oils, deposit onto the wellbore surface, block the production facilities, and result in unexpected downtime. The consequences of inadequate management of asphaltene issues could lead to an approximate loss of $1.2 MM/day due to discontinued production and an estimated cost of $0.5−3 MM for removal of deposits.[3]

Asphaltenes are indigenous molecules in crude oil, known to be one of the most polar and surface-active components. By definition, asphaltenes are soluble in aromatic hydrocarbons but insoluble in alkanes. During the recovery process, crude oils flow from the reservoir to the surface, and the fluid temperature and pressure decrease with the height. The solubility of the fluid mixture in the field decreases, so asphaltene molecules become unstable and precipitate out. After reaching the bubble point pressure, as the fluid pressure and temperature decrease further, the mixture solubility increases due to the escape of light-end hydrocarbons from the liquid mixture. After the fluid pressure reaches a certain point, asphaltenes become stable again in the mixture, and no more asphaltenes precipitate from the blend.[2,4] The solvent solubility power is believed to be the key factor in studying the onset of asphaltene precipitation and the formation of asphaltene deposits in the instability zone.

Yet, the asphaltene deposition problem is not completely the same as the asphaltene precipitation problem. A range of laboratory tests and theoretical models are available to identify and predict the onset point of precipitation. The laboratory techniques, including but not limited to the gravimetric precipitation method,[4,5] acoustic resonance,[4,6] and solid detection using optical microscopy or high-pressure microscopy,[4,7−11] provide a primary source to help understand asphaltene precipitation problems at the field conditions. However, the onset conditions might be different for precipitation and deposition. A recent study[12] confirmed that the instantaneous precipitation onset point was irrelevant to the deposition process and found that the accumulation of submicrometer asphaltene aggregates led to the deposition. Moreover, the amount and rate of deposition are not necessarily correlated with the precipitated amount and rate of asphaltene precipitation, which is frequently observed in most onset pressure tests.

Received: February 29, 2020
Revised: June 29, 2020
Published: July 2, 2020

Table 1. Measured Density and Viscosity of Samples at Temperature of 20 °C and Shear Rate of 100 $s^{-1}$

| | dilution ratio (v:v) (in pure toluene) | | | | | |
|---|---|---|---|---|---|---|
| | 1:100 | 1:50 | 1:20 | 1:4 | 1:1 | 1:0.25 |
| density ($g/cm^3$) | 0.8670 | 0.8672 | 0.8677 | 0.8705 | 0.8768 | 0.8846 |
| viscosity (mPa·s) | 0.602 | 0.629 | 0.700 | 0.948 | 2.370 | 12.382 |

| | hep/tol volume ratio (dilution ratio = 1:20) | | | | |
|---|---|---|---|---|---|
| | 50:50 | 60:40 | 70:30 | 80:20 | 90:10 |
| density ($g/cm^3$) | 0.7808 | 0.7629 | 0.7458 | 0.7282 | 0.7108 |
| viscosity (mPa·s) | 0.565 | 0.542 | 0.534 | 0.527 | 0.513 |

| | hep/tol volume ratio (dilution ratio = 1:1) | | | | |
|---|---|---|---|---|---|
| | 50:50 | 60:40 | 70:30 | 80:20 | 90:10 |
| density ($g/cm^3$) | 0.8332 | 0.8241 | 0.8155 | 0.8071 | 0.7991 |
| viscosity (mPa·s) | 2.132 | 2.108 | 2.209 | 2.251 | 2.613 |

Adsorption of asphaltenes on a wide variety of solid surfaces has been explored in the literature, including but not limited to mineral (clay,[13−15] sandstone,[16−18] silica,[19,20] quartz,[21,22] mica,[23−26] dolomite,[16,27−29] montmorillonite[30]), metal (aluminum,[31,32] gold,[32−35] and iron[31,33,36,37]), metal oxides, and stainless-steel surfaces.[32,38] Langmuir-type isotherms were reported in most studies[18,39−41] when the asphaltene concentration was low or the surface had poor affinity to asphaltenes. Previous work on investigating asphaltene deposition using X-ray photoelectron spectroscopy identified different functional groups of asphaltene molecules in the single adsorbed layer and found that there was little difference in their binding energies with the metal surface.[38]

The quartz crystal microbalance with dissipation (QCM-D) technique is believed to be a promising tool to study the adsorption of asphaltenes onto solid surfaces. To evaluate the adsorption kinetics of more complex mixtures, Tavakkoli et al.[42] studied crude oil asphaltene deposition under flow conditions by varying the ratio of heptane/toluene and showed that the precipitation onset happened near 75 vol% heptane[42] for their particular oil. The deposited asphaltenes were found to first increase until the precipitation onset point and then decrease with the heptane content. The authors proposed a transient model to describe the transport of asphaltenes in the QCM-D chamber after asphaltenes started to precipitate, which involved different processes, including precipitation, aggregation, diffusion, advection, and deposition.[42] In terms of numerical modeling, the perturbed-chain statistical associating fluid theory (PC-SAFT)[43] is believed to be a promising equation of state to predict the precipitation of asphaltenes in the wellbore at high temperature and pressure conditions. However, the PC-SAFT model is very sensitive to the accuracy of measurements of the precipitated asphaltenes.[44] Another possibility is a parametric scaling model based on transport and diffusion-driven deposition by fitting with experiment results of precipitating asphaltenes solution passing through metal pipes at different flow conditions.[45] Nevertheless, the interaction between the metal surface and the deposited molecules was not taken into consideration. Ekholm et al.[34] studied the adsorption of re-dissolved asphaltenes from heptane/toluene mixtures onto gold surfaces and found that, at low concentration, adsorbed asphaltene molecules form a rigid layer; at higher concentration, due to the formation of aggregates in bulk concentration, the amount of adsorption increases further. However, the kinetics of deposit formation was not fully explored, and the correlation between the concentration and deposition was missing. For even higher concentrations, there are very limited studies available, and research using real crude oil is even less due to the complexity of its composition. Despite extensive experimental and theoretical studies on asphaltene−metal interactions, there is not so much information available on asphaltene deposition kinetics, and the underlying physics of asphaltene deposition mechanisms is still poorly understood. The deposition kinetics, the effect of solvent solubility, and the mechanism of asphaltene depositions all need further investigation.

To mitigate or remediate the asphaltene problem, asphaltene inhibitors or dispersants are used in the oilfields. A series of laboratory screening tests have been developed and studied to evaluate their performance.[46−48] The most common methods involve precipitation tests using large relative volumes of heptane and measuring, directly or indirectly, the resultant particle size of the flocculates. The formation of fewer and smaller flocculates from such a test indicates success of the selected inhibitor. However, these screening tests do not test for deposition but only for precipitation. Results from laboratory screening do not readily transfer to field performance. It has been validated in earlier studies[42,49,50] that QCM-D is sensitive to detect the adsorbed asphaltene films and has been shown as a promising tool for testing the efficiency of the commercial inhibitors for depositions.

In the work described in this paper, we conducted an experimental investigation of crude oil asphaltene depositions onto stainless-steel surfaces using the quartz crystal microbalance with dissipation technique and studied the effect of asphaltene concentrations and solvent solubility in the formation of asphaltene deposits. We illustrated the potential of the QCM-D technique as a lab screening tool for selecting asphaltene inhibitors to help remediate the deposition problems. We aim to understand how asphaltenes deposit onto the stainless-steel surface for better management of asphaltene problems in upstream crude oil production.

## 2. EXPERIMENTAL SECTION

In the crude oil production system, due to the changes in temperature and pressure, the solubility of the oil blend decreases during the depressurization process so that asphaltenes start to precipitate and deposit onto the components of the production facilities. In order to study the effect of the solubility change, in our experimental setup, we are using a heptane/toluene solvent mixture at different mixing ratios


https://dx.doi.org/10.1021/acs.energyfuels.0c00663
Energy Fuels XXXX, XXX, XXX−XXX

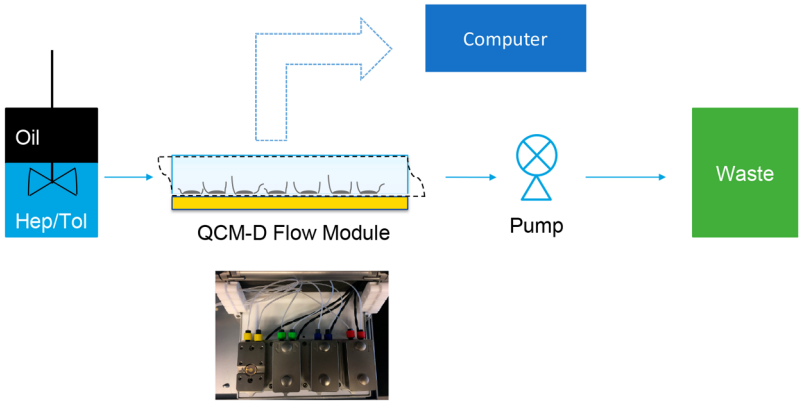


**Figure 1.** Schematics of experimental setup.

to achieve the same solubility that is present during the depressurization process.

**2.1. Materials.** The crude oil sample used in this study is stock-tank oil with a density of 0.8909 g/cm$^3$, viscosity of 115.18 mPa·s, and asphaltene content of 4 wt%. The solvents, toluene (99.8+%, ACROS Organics) and *n*-heptane (HPLC-grade, submicron filtered, Fisher Chemical), are directly used without further purification. Millipore water is used for cleaning and rinsing, and high-purity nitrogen (Gasco, part no. 10L-114) is applied for drying at the end of cleaning procedure.

**2.2. Sample Preparations.** For each experiment, the crude oil sample is first heated to 60 °C for 10−15 min. This is to dissolve the wax fractions that have precipitated due to the low temperature and to facilitate the flow of viscous crude oil in the following sampling procedure. Next, the heated sample is diluted at a certain ratio by the heptane/toluene solvent mixture, and the mixture is kept stirred on a heated stirring plate. This step should be completed just before the mixture solution is pumped into the QCM flow module at a certain flow rate in order to avoid early precipitation.

**2.3. Measurement of Density and Viscosity.** As the composition of the crude oil sample is unknown, the density and viscosity of crude oil samples and prepared sample solution need to be measured for each test. After the sample is freshly prepared, its density is measured at a shear rate of 3500 s$^{-1}$ using an Anton Paar Stabinger Viscometer SVM 3000 (viscosity range: 0.2−20 000 mPa·s, temperature range: −56 to 105 °C). The viscosity of the sample is measured through flow sweep tests in parallel-plate configuration using a Discovery H-3 hybrid rheometer. The measured properties are summarized in Table 1.

**2.4. QCM-D Experiment.** The instruments used in the QCM-D experiments include but are not limited to an Ismatec peristaltic pump, Tygon tubes, a Kalrez O-ring sealing gasket, and a QSense analyzer (Nanoscience Instruments, temperature range: 15−65 °C). The acquired experimental data are analyzed by QSense Dfind software (Nanoscience Instruments) and in-house developed Mathematica tools.

In the production well, the most common well casing materials are carbon steel, plastic, and stainless steel, depending on the geological formations. In our application, a sensor with a stainless-steel surface coating (SS2343) is selected for the experimental study, and the surface roughness is less than 1 nm RMS.

The disposable stainless-steel-coated quartz crystal is pre-cleaned before the experiment, as the QCM-D technique is based on the frequency resonance change and any contaminants attached to the sensor surface will greatly affect the accuracy of the experiment. First, the sensor is placed near the lamp in a UV/ozone ProCleaner PLUS system for 5−10 min. The sensor surface is treated with UV light at a wavelength of 254 nm as well as the ozone generated by the UV wavelength at 184 nm. This is to decompose the deposited organics into volatile substances by ultraviolet rays and strong oxidation so that they can be removed from the contaminated surfaces. Second, deionized water is used to rinse the sensor several times, and the sensor is then gently blow-dried under a flow of nitrogen gas. Last, the sensor is placed back to the UV/ozone chamber for another 10 min treatment.

The setup of the QCM-D experiments is illustrated in Figure 1, and the following procedure is performed in each experiment. First, the cleaned crystal sensor is mounted in the measurement chamber modules. The experiment is set to run at normal temperature and pressure, i.e., 20 °C and 1 atm. The reference solvent or solvent mixture is pumped through the module at a speed of 50 $\mu$L/min until a stable baseline is achieved. The inlet is then switched to the freshly prepared samples that are kept stirring and run for a certain time period. The variations of resonance frequency and the energy dissipations during oscillations are measured, recorded, and transmitted to the computer. The waste is collected at the end of the peristaltic pump.

After each experiment, the flow module and the connecting tubing are flushed according to the relevant cleaning protocol and the used sensor is disposed of.

**2.5. Principle of QCM-D.** The QCM-D system allows real-time kinetic analysis of adsorbed mass and viscoelastic properties of adsorbed films. It can be used to study the adsorption through measurement of mass changes with time and rigidity/softness changes of the film formed on the coated crystal surface. This feature enables QCM-D to detect a transition from a monolayer to an aggregate multilayer and analyze adequately adsorption kinetics/experiments.

The primary configuration for QCM-D experiments begins with adsorption from a liquid phase (either stagnant or flowing, with variable composition) onto a clean solid surface of variable properties (e.g., density and strength of exposed cations/anions depending on the coating surface) to study variations of adsorption kinetics/equilibrium in the monolayer/multilayer regime. Using the energy dissipation capability of the QCM-D technique, one can determine if the adsorbed film is rigid or viscoelastic, which is not possible looking only at the frequency response. In addition to such structural analysis, QCM-D also allows real-time kinetic analysis of both mass and viscoelastic changes.

The controlling unit in the QCM-D technique is the quartz crystal sensor, which oscillates when the given frequency reaches the intrinsic resonance frequency of the quartz sensor. If molecules adsorb onto the sensor surface, they will bind with the sensor and oscillate together with the sensor. The frequency of the system will decrease due to the increase in its mass. For molecules that are rigidly attached to the sensor surface, there is no slip of the deposited molecules on the crystal surface, and hence there is no dissipation in the oscillations. In this case, one can apply the Sauerbrey equation and calculate the amount of adsorbed mass density from the measured frequency change:[51]

$$\Delta m = -\frac{C}{n}\Delta f \tag{1}$$


https://dx.doi.org/10.1021/acs.energyfuels.0c00663
Energy Fuels XXXX, XXX, XXX−XXX

where $C$ is a constant of the quartz crystal (i.e., 17.7 ng/(Hz·cm$^2$) for a 5 MHz crystal) and $n$ is the number of the overtone. This is valid when the adsorbed mass is small compared to the crystal itself and the adsorbed molecules are assumed to be evenly distributed.

In addition to the adsorption of molecules, the liquid that transports the solid molecules through the flow module and the liquid that is trapped inside the adsorbed molecules also contribute to the change of frequency.[51−53] The frequency change due to liquid loading can be calculated from

$$\Delta f_{\text{liq-load}} = -\sqrt{\frac{n}{\pi}}\frac{f_0^{3/2}}{\rho_q \nu_q}\left(\sqrt{\rho_l \eta_l} - \sqrt{\rho_s \eta_s}\right) \tag{2}$$

$$\Delta D_{\text{liq-load}} = \frac{1}{\sqrt{n\pi}}\frac{2f_0^{1/2}}{\rho_q \nu_q}\left(\sqrt{\rho_l \eta_l} - \sqrt{\rho_s \eta_s}\right) \tag{3}$$

where $f_0$ is the fundamental frequency of the quartz crystal, $\rho_q$ is the specific density of the quartz crystal, and $\nu_q$ is the shear wave velocity in quartz. The subscripts "l" and "s" refer to liquid mixture and pure solvent, respectively. It can be observed from eqs 2 and 3 that $\Delta f_{\text{liq-load}}/\Delta D_{\text{liq-load}} = -nf_0/2$. In other words, if this relation holds true in the experimental data, the effect of liquid trapping can be considered as negligible.

## 3. RESULTS AND DISCUSSION

**3.1. Validation of the QCM-D Experiment.** The effect of introducing a liquid mixture into the QCM-D chamber has been discussed earlier.[42,49] Pure solvent mixtures composed of heptane and toluene at different ratios have been tested using the previously described experimental procedure. The acquired frequency change and dissipation data are plotted against the calculated values from Sauerbrey equation for comparison.

As can be seen from Figure 2, the measured frequency change and dissipation data agree well with the corresponding values calculated from the Sauerbrey equation. The percent errors all fall within the range of ±3%. This confirms the applicability of the equation for liquid loading and validates the use of the QCM-D technique with the current experimental setup. All the direct measurements from QCM-D experiments will have to be processed with the exclusion of the variation in frequency due to the density and viscosity change of the fluid after the inlet is switched to the sample in the data analysis.

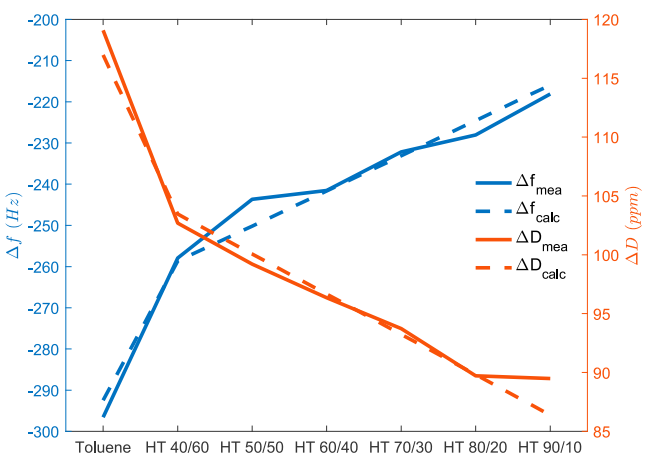


**Figure 2.** Validation of frequency change and dissipation using solvent mixture with various heptane/toluene ratios. H stands for heptane; T stands for toluene; HT4060 refers to the solvent mixture with 40% in volume as heptane and 60% in volume as toluene.

**3.2. Adsorption of Crude Oil in Toluene on a Stainless-Steel Surface.** The adsorption kinetics curves of crude oil in toluene solutions are shown in Figure 3. It can be observed that the amount of adsorbed mass increases with time, regardless of the toluene content. The adsorption initially undergoes a rapid increase and then slows down to asymptotically approach the equilibrium. With decreasing toluene in the sample mixture, the adsorption reaches equilibrium faster since there are more asphaltene molecules available for adsorption.

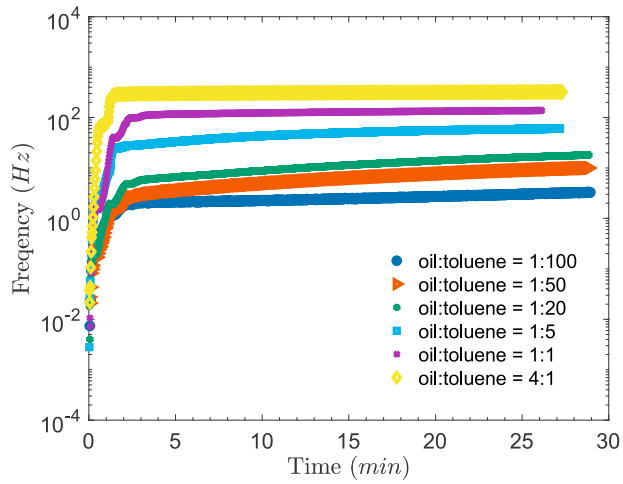


**Figure 3.** Adsorption kinetics of crude oil in pure toluene at different dilution ratios.

To get an idea of how asphaltenes start to deposit onto the solid surface, the adsorption kinetics data in the rapidly increasing regime further will be analyzed. After the initial rapid increase, most of the adsorption kinetics curves for the crude oil in toluene solution exhibit an undulate shape (see Figure 4). As time proceeds, the kinetics curve tends to level off for a short period (several seconds) and then continues its growth toward the equilibrium, especially at low asphaltene concentrations. One could attribute these variations in the surface adsorption to the peristaltic pump, which introduces oscillatory waves. However, this hypothesis does not explain

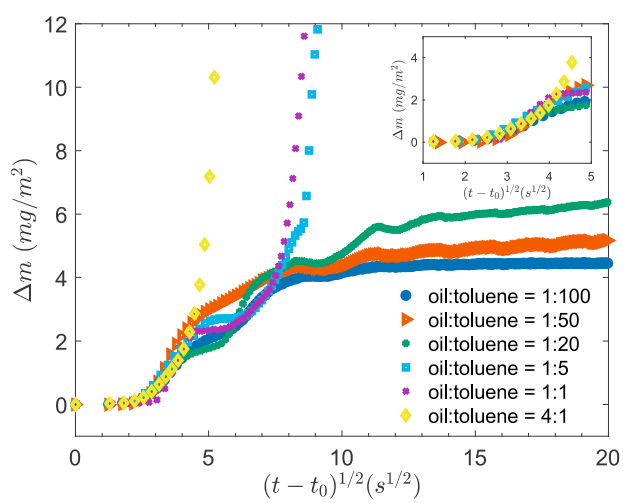


**Figure 4.** Dynamic adsorption versus square root of time for crude oil in toluene with different dilution ratios.


https://dx.doi.org/10.1021/acs.energyfuels.0c00663
Energy Fuels XXXX, XXX, XXX−XXX

the relatively quiescent and stable frequency signals measured in the long term. Another possible explanation is proposed in section 3.4, based on our observations from the QCM-D experiments. It can also be observed that, at low concentrations, the adsorption seems to reach a plateau within a few minutes, and the adsorbed mass is in the range of 4−6 mg/m$^2$, which corresponds to a monolayer adsorption regime, as reported in the literature.[13,33,35,49,54−56] For higher concentrations, the adsorbed mass blows up within several seconds and goes beyond a much higher value.

**3.3. Initial Diffusion-Controlled Kinetics.** From the close-up subplot of the initial several seconds inside Figure 4, the mass change for all concentrations was found to vary linearly with the square root of time, which implies a diffusion-controlled process. Using the classical Ward and Tordai equation[57] for surfactant diffusion, the time variation of the surface concentration can then be calculated:

$$\Gamma(t) = 2\sqrt{\frac{D}{\pi}}\left(C_b\sqrt{t} - \int_0^{\sqrt{t}} C_s(\tau)\, d\sqrt{t-\tau}\right) \quad (4)$$

where $\Gamma$ is the surface coverage of the adsorbed molecules at the surface, $D$ is the diffusion coefficient, $C_b$ is the bulk concentration, and $C_s$ is the concentration in the subsurface layer. At short times, the second term in the equation that accounts for desorption can be considered as negligible, and the surface concentration only varies linearly with the square root of time:

$$\Gamma = C\sqrt{\frac{Dt}{\pi}} \quad (5)$$

The apparent diffusion coefficient, which could be estimated from the slope of the $\Gamma$ versus $t^{1/2}$ curve at the initial several points, is a function of concentration:

$$S = 2C\sqrt{\frac{D}{\pi}} \quad (6)$$

where $C$ is the bulk concentration of asphaltene molecules. Assuming the adsorbed molecules have a spherical shape, the hydrodynamic diameter of the particles can be then approximated using the Stokes−Einstein equation for steady-state flow:

$$d = \frac{k_B T}{3\pi\eta_s D} \quad (7)$$

where $k_B$ is the Boltzmann constant ($1.38 \times 10^{-23}$ m$^2$·kg/(s$^2$·K)), $T$ is the temperature, and $\eta_s$ is the viscosity of the surrounding fluid.

Extracting the slope of the initial adsorption kinetics curve and implementing that into the above equations, the diameters of the adsorbed species for crude oil in toluene at different dilution ratios were then estimated (see Table 2) and are plotted in Figure 5. At low concentrations (<1 kg/m$^3$), the adsorbed molecules have an approximate diameter of several hundred nanometers; when the samples become more concentrated (>10 kg/m$^3$), the diameter could go up to tens of micrometers, in line with the reported values,[58] indicating the formation of larger asphaltene aggregates on the solid surface. The last data point of the adsorbed molecular size at high concentrations seems not to follow the trend of increasing with concentration. This might contribute to the agglomeration/flocculation of asphaltenes.[59−61] When the size of the aggregates goes beyond a certain point, instead of depositing, the large floc precipitates and flows through the cell due to the inertial forces. A similar behavior was also observed and explained in earlier studies.[42,62,63]

**Table 2. Estimated Size of Adsorbed Species**

| dilution ratio (v:v) | $C_{asph}$ (kg/m$^3$) | slope (×10$^7$ kg·m$^{-2}$·s$^{-1/2}$) | $D$ (×10$^{15}$ m$^2$/s) | $d$ ($\mu$m) |
|---|---|---|---|---|
| 1:100 | 0.356 | 8.63 | 4610 | 0.154 |
| 1:50 | 0.713 | 13.33 | 2750 | 0.254 |
| 1:20 | 1.782 | 8.08 | 161 | 3.840 |
| 1:5 | 7.127 | 9.68 | 14.5 | 31.582 |
| 1:1 | 17.818 | 14.32 | 5.08 | 36.046 |
| 4:1 | 28.509 | 26.60 | 6.83 | 5.130 |

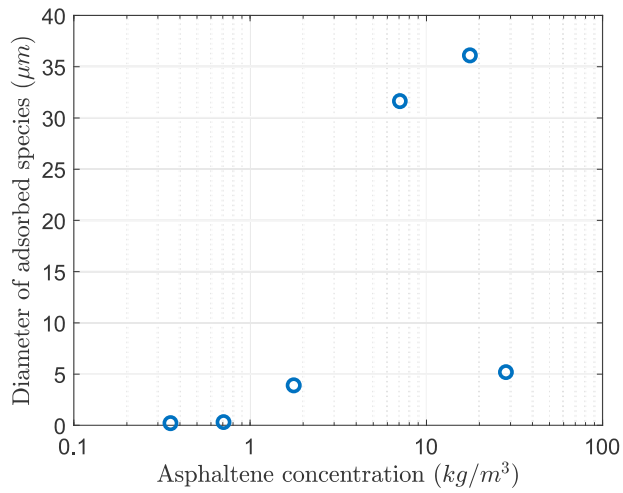


**Figure 5.** Estimated adsorbed particle size from the initial diffusion-controlled adsorption kinetics at different asphaltene concentrations.

**3.4. Transition to Multilayer Adsorption.** The dissipation change is plotted against the frequency change in Figure 6. It was observed that all the curves fall into almost the same straight line regardless of dilution ratios, and the slopes of the curves for lower asphaltene concentrations are approximately the same as the ones calculated in the cases of pure

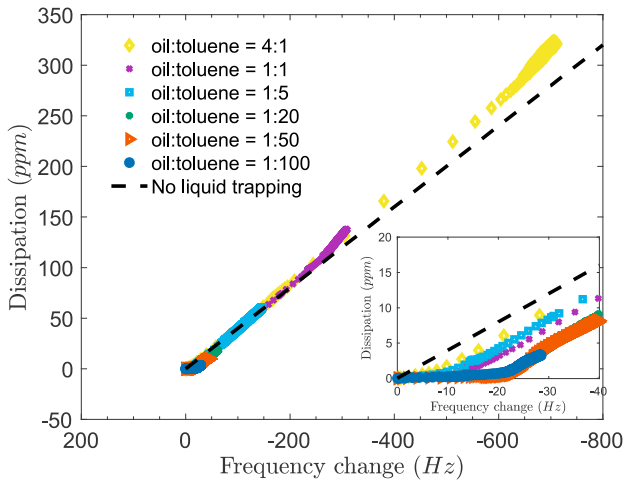


**Figure 6.** Dissipation versus frequency change plot for crude oil in toluene solution at different dilution ratios. The subplot on the bottom right shows a close-up at the frequency change from 0 to −40 Hz.


https://dx.doi.org/10.1021/acs.energyfuels.0c00663
Energy Fuels XXXX, XXX, XXX−XXX

liquid loading and mass loading without liquid trapping effect. The correspondence of the multiple $D-f$ curves indicates that the molecules adsorbed from crude oil solutions at low asphaltene concentrations form films with similar structures or properties. Nevertheless, for higher asphaltene concentrations (i.e., lower dilution ratios), there appears to be two regions where the $D-f$ curve tends to have different slopes. The adsorbed molecules seem to first build films similar to that formed at low asphaltene concentration, which is indicated by the same slope. At some point, the $D-f$ curves then start to deviate from the theoretical one without liquid trapping effect and continue growing, with a larger ratio of $\Delta D$ over $-\Delta f$. This suggests that, after reaching a certain critical point, the adsorbed molecules start to form a film with structure different from that in the previous process. The higher dissipation values seem to indicate an increase in the formation of voluminous and loose aggregates and the inclusion of solvent inside the adsorbed films on the solid surfaces with time.

When plotting the ratio of $\Delta D/-\Delta f$ versus the adsorbed mass (see Figure 7), it was found that the ratio of $\Delta D$ over

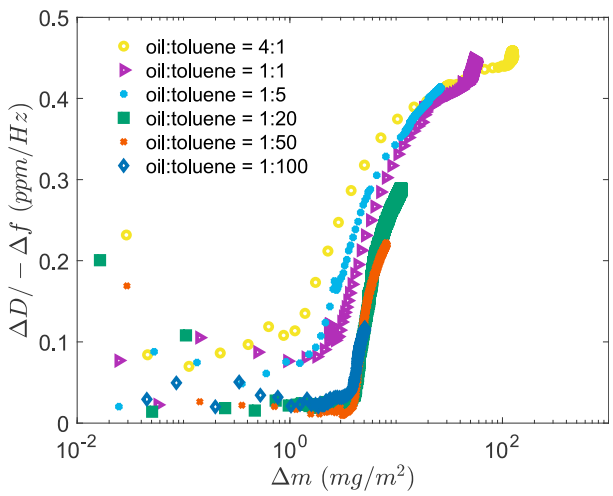


**Figure 7.** $\Delta D/-\Delta f$ ratio versus the adsorbed mass at different dilution ratios.

$-\Delta f$ was initially independent of surface coverage and then significantly increased until it reached a plateau. For highly concentrated solutions, this feature is repeated in the next cycle, where the adsorbed mass keeps growing.

This could further be explained by a two-step deposition model, which was originally proposed for amphiphile adsorption from organic solvents to liquid/solid interfaces by Zhu and Gu (i.e., the ZG model).[64] Based on the two-step adsorption model (see Figure 8), first, asphaltene monomers adsorb through the interaction between the $\pi$-electrons of the polyaromatic hydrocarbon rings and the hydrophilic surfaces. This has been advocated by the interactions between polyaromatic hydrocarbons[65] and asphaltene adsorption at the water−oil interface.[66] This step could lead to the formation of a Langmuir monolayer adsorbed on the solid surface, and the mechanism is similar to that of asphaltene adsorption onto the liquid/liquid interface found in previous studies.[61,66−72] Next, the adsorption increases significantly as aggregates start to form on several active sites through the interaction between the freshly adsorbed molecules and the molecules that were adsorbed earlier in the first step. The binding energy between the already adsorbed and the next layer of adsorbing molecules

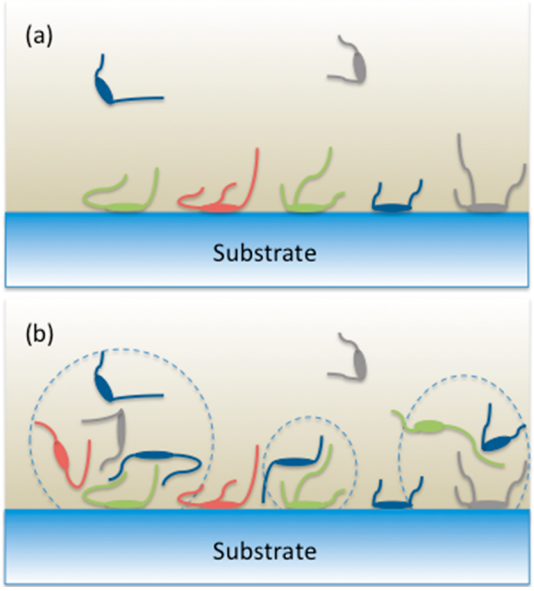


**Figure 8.** Illustration of the two-step adsorption model. (a) Asphaltene monomers adsorb onto the substrate. (b) Asphaltene molecules adsorb onto the previously adsorbed molecules and form nanoaggregates.

significantly decreases due to the weak interactions between the alkyl chains of the polyaromatic hydrocarbons and the physisorption of the aggregates, which tend to be voluminous and loose. This implies the possibility of a large space between the adsorbed molecules, which could accommodate and trap more fluid and hence increase the dissipation during oscillations.

This two-step adsorption model was justified to be applicable to asphaltene molecules because asphaltene molecules tend to adsorb onto a liquid/liquid interface or aggregate in the solution due to their amphiphilic characteristics.[66] The model was shown to be successful to fit with experimental data in an earlier study on asphaltene adsorption from toluene onto some reservoir rock surfaces such as dolomite and Berea sandstone.[16] The ZG model proved accurate to predict the adsorption amount in the concentration range up to 30 000 ppm,[16] and the adsorption isotherm is calculated according to[64]

$$\Gamma = \frac{\Gamma^{\infty} k_1 C\left(\frac{1}{n} + k_2 C^{n-1}\right)}{1 + k_1 C(1 + k_2 C^{n-1})} \quad (8)$$

where $\Gamma$ is the amount of adsorbed molecules, $\Gamma^{\infty}$ is the maximum possible adsorption at high concentrations, $k_1$ is the first adsorption step parameter, i.e., the adsorption of asphaltenes in solution to the solid surface, $k_2$ is the second adsorption step parameter, i.e., the adsorption of asphaltenes in solution to those asphaltene molecules that have already adsorbed to the solid, $C$ is the bulk concentration, and $n$ is the mean aggregation number of the adsorbed molecules. When the second adsorption step parameter, i.e., $k_2$, becomes negligible, the above equation becomes a Langmuir-type adsorption isotherm. By implementing the two-step deposition model (i.e., the ZG model)[64] and fitting with the experimental data, the maximum surface coverage and the adsorption parameters could be numerically computed in the optimization process.


https://dx.doi.org/10.1021/acs.energyfuels.0c00663
Energy Fuels XXXX, XXX, XXX−XXX

The adsorbed mass from asphaltene solutions at different concentrations is plotted in Figure 9, with the fitting curves

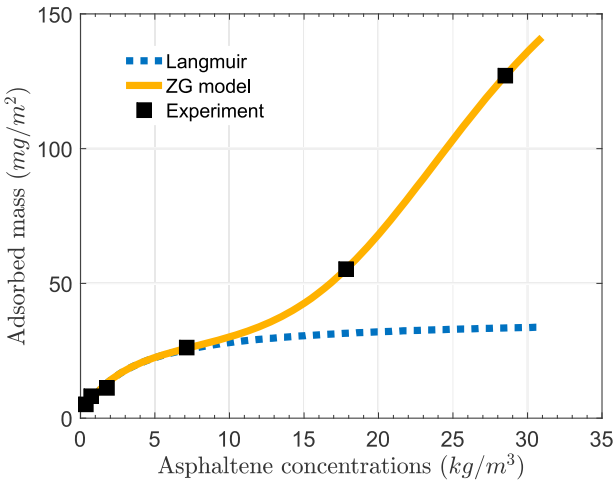


**Figure 9.** Adsorption isotherm of crude oil in pure toluene as a function of asphaltene concentration.

generated from the two-step deposition model (i.e., ZG model) and the Langmuir monolayer case using the optimized adsorption parameters and the maximum mass surface coverage. As observed from the figure, the adsorbed mass shows an increasing trend as the asphaltene content increases, and it exhibits multiple regions with different characteristics. After a rapid increase with asphaltene content, the adsorbed mass does not reach the equilibrium and the change of adsorbed mass slows down, but later the mass builds up quickly again with increasing concentration. It seems that after reaching a certain critical asphaltene concentration, the adsorbed films would go through a transition from monolayer to multilayer adsorption of asphaltene molecules. The Langmuir curve fits well with the experimental data until 9000 ppm and then levels off with increasing concentration, while the ZG model agrees well with the experimental data at both low and high concentrations. The ZG model is particularly consistent with the transition behavior from monolayer to multilayer adsorption. The obtained mean aggregation number of adsorbed molecules is 5.28, which is quite consistent with the values for Bedford limestone and dolomite rock reported in a previous study.[16] To get an idea of how the adsorbed films look like, the sensor surfaces were scanned under a microscope after 30 min asphaltene adsorption. As shown in Figure 10, at higher concentrations, the deposited molecules formed thick films with uniformly distributed dark spots; at lower concentrations, they only formed a thin film layer, which can barely be seen from the image. In a recent study,[73] optical images of the gold surface were obtained after 24 h immersion in oil with heptane using confocal microscopy and laser scanning, and they showed similar results. The multiple dotted regions indicate the presence of active sites and the corresponding adsorbed complex.

**3.5. Comparison with Different Surfaces.** Previous studies[34,39,42,49] have shown that crude oil dissolved in pure toluene could adsorb onto different coating surfaces. Compared with the deposited mass on different types of surfaces reported in the literature, our values seem to be

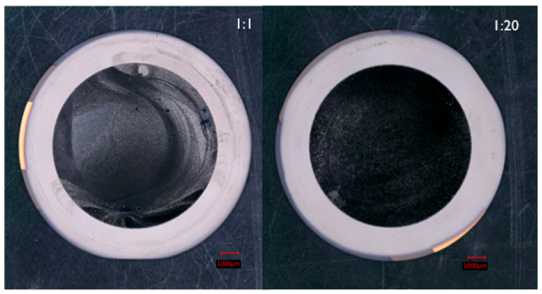


**Figure 10.** Microscope images of stainless-steel-coated quartz surface after 30 min asphaltene adsorption. On the left, the dilution ratio of oil to toluene is 1:1; on the right, the dilution ratio of oil to toluene is 1:20.

comparable in the lower concentration range (see Figure 11 and Table 3).

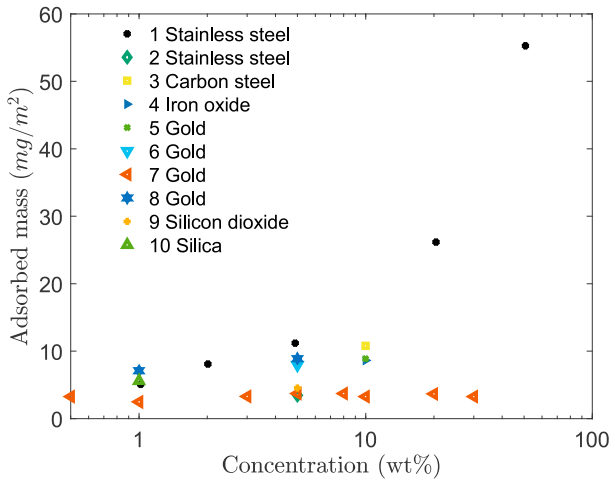


**Figure 11.** Comparison with the values of asphaltene adsorption on different surfaces reported in the literature.[34,35,42,49,74]

**Table 3. List of QCM-D Studies on Different Coating Surfaces Using Crude Oil Samples**

| no. | surface | crude type | solvent | asph (wt%) | reference |
|---|---|---|---|---|---|
| 1 | stainless steel | EM crude | toluene | 4.0 | current study, 2019 |
| 2 | stainless steel | Tensleep crude | toluene | 3.2 | Abudu and Goual, 2009 |
| 3 | carbon steel | crude oil (S) | heptane | 2.8 | Tavakkoli et al., 2014 |
| 4 | iron oxide | crude oil (S) | heptane | 2.8 | Tavakkoli et al., 2014 |
| 5 | gold | crude oil (S) | heptane | 2.8 | Tavakkoli et al., 2014 |
| 6 | gold | Cold Lake bitumen | toluene | 59.5 | Zahabi et al., 2012 |
| 7 | gold | Tensleep crude | toluene | 3.2 | Abudu and Goual, 2009 |
| 8 | gold | North Sea crude | 50:50 hep/tol | 2.9 | Ekholm et al., 2002 |
| 9 | silicon dioxide | Tensleep crude | toluene | 3.2 | Abudu and Goual, 2009 |
| 10 | silica | Brazilian heavy crude | toluene | 10.2 | Hannisdal et al., 2006 |


https://dx.doi.org/10.1021/acs.energyfuels.0c00663
Energy Fuels XXXX, XXX, XXX−XXX

For higher concentrations, there are very limited data available on crude oil samples. On one hand, the adsorbed mass measured from the experiment does not show any clear correlations with the surface coating type. On the other hand, as the concentration of crude oil increases, the adsorbed mass starts to deviate from the monolayer adsorption regime from very low concentration and then significantly increases with increasing concentration. This observation could be explained by the proposed multilayer adsorption mechanism. After asphaltene molecules interact with the solid surface, the following step is mainly through the interaction between the first layer of the adsorbed asphaltene molecules and the subsequent asphaltene molecules in the bulk solution that diffuse to the surface. The structure or molecular orientation of the initially deposited asphaltene molecules might be altered due to the bonding energy difference of various solid surfaces, which results in a widely distributed surface or functional groups from the previously deposited molecules available at the surface. Nonetheless, the observed slight difference in the amount adsorbed at different coating surfaces seems to confirm that the deposition shows little dependence on the nature of the surface but instead probably relies on the interactions between asphaltene molecules in the subsequent adsorption step. The remarkable increase in the deposition amount at higher concentration could probably be attributed to the presence of resins and other compositions of crude oils, which could form a large and complex system with asphaltene molecules and decrease their solubility.[34] One may notice that some types of crude oils at high concentrations adsorb onto the solid surfaces and form a monolayer,[49] while others adsorb in multilayers. This difference might be caused by the difference in the heteroatoms such as sulfur or surface-active groups in the asphaltene molecules.[62] Instead of interacting with the solid surface, these groups of molecules are likely to self-associate, which would lead to the decrease in the number of surface-active molecules that are available for adsorption.[62] The polydispersity in crude oil composition also adds to the complexity of the adsorption problem.[56]

**3.6. Effect of Solvency.** To investigate how the solvent solubility affects asphaltene deposition, the samples were prepared by mixing crude oil and the solvent mixture composed of heptane and toluene at different volume ratios. The dilution ratios of crude oil to solvent mixture used here are 1:20 and 1:1 so that the solvency effect at low and high concentrations can be compared.

The adsorbed mass after 2 h adsorption is plotted against the volume fraction of heptane in Figure 12 for both dilution ratios. Theoretically, as the percentage of heptane increases in the mixture, the solvent solubility for asphaltenes will decrease until it reaches a critical point where asphaltenes become unstable and start to precipitate out from the solution. Previous studies[7,48,75−77] have revealed the accumulation in the amount of precipitates with heptane increment. To the contrary, our experimental results showed that the amount of deposition after 2 h adsorption does not monotonically increase with heptane content. Instead, from the point beyond 50 vol% heptane content, it seems that the adsorbed mass first increased to a maximum value and then exhibited a decreasing trend as the heptane content increased. This bell-shaped curve was observed for both low and high dilutions and was also reported in an earlier study of crude oil adsorption onto gold surfaces.[42,63,78] The asphaltene fraction that has precipitated out at the solubility with 70 vol% heptane content seems to be

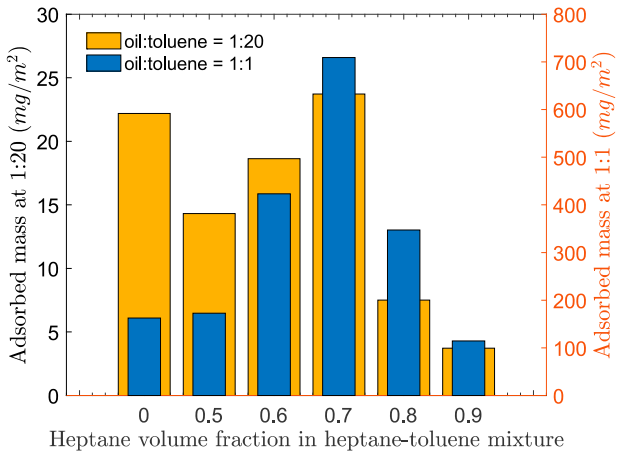


**Figure 12.** Adsorbed mass plotted as a function of heptane fractions at different dilution ratios.

the fraction that produces the largest deposition. From an earlier study of asphaltene solubility fractions using fluorescent depolarization technique,[79] it was found that different solubility fractions have the same molecular species but differ in the amount of each species. Asphaltenes tend to form aggregates even in a good solvent.[80] Upon decreasing the solvent aromaticity, the asphaltene aggregates grow in average size and molecular weight along with the increasing heptane content,[77,79,81,82] and the adsorbed film thickness increases with the size of aggregates in the solution.[83] The average aggregate size continues to grow until the solution reaches the solubility limit, above which the addition of heptane would lead to significant agglomeration and precipitation, leaving smaller asphaltene aggregates in the solution.[77] As explained in the previous section, asphaltene molecules adsorb onto the solid surface through the interaction between their $\pi$-electrons and the hydrophilic surface, and they tend to expose their nonpolar parts to the oil phase in bad solvent conditions (i.e., higher percentage of heptane),[26] which would potentially interact with the alkyl chains of the asphaltene aggregates in the solution. This is highly dependent on the aggregate size, because large aggregates with a size exceeding a certain value did not appear to adsorb at the interface.[54] It could be inferred that the percentage of the molecular species that form aggregates with the optimal size reaches the maximum in the solubility fraction at 70 vol% heptane content and these aggregates are the most prone to interact with the adsorption sites.

On the other hand, at lower concentration, the precipitated asphaltene aggregates at higher heptane fraction seem to have less affinity to the solid surface or active sites, as most of the precipitated mass was carried out by the flowing solvent without depositing onto the solid surface, as implied by the measured small amount of adsorption (Figure 12) and low dissipation values (Figure 13). When the heptane volume fraction goes beyond 70% by volume, the dissipation becomes less than 10 ppm, indicating that the adsorbed films are rigid. Compared to the lower concentration, i.e., the dilution ratio of 1:20, the amount of adsorption and the dissipation values at the dilution ratio of 1:1 are much higher (see Figure 14). At higher concentrations, the dissipation values with heptane addition ranged from 220 to 280 ppm, almost the double of the values for pure toluene. This suggests that with less toluene in the mixture, the increase in the heptane content could lead


https://dx.doi.org/10.1021/acs.energyfuels.0c00663
Energy Fuels XXXX, XXX, XXX−XXX

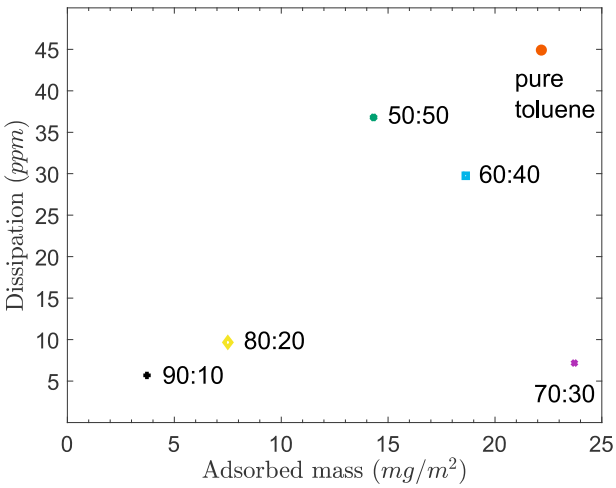


**Figure 13.** Dissipation change versus the adsorbed mass plot for crude oil in solvent mixture with different heptane/toluene ratios (dilution ratio is 1:20).

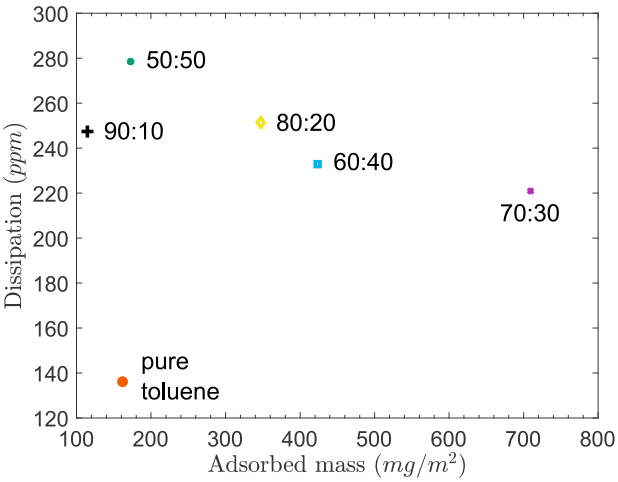


**Figure 14.** Dissipation change versus the adsorbed mass plot for crude oil in solvent mixture with different heptane/toluene ratios (dilution ratio is 1:1).

to a totally different composition of molecular species and mean aggregate size at different dilution ratios. At higher concentration, with the addition of the flocculants, i.e., heptane, the adsorbed films would be more voluminous and viscoelastic.

These observations in the study of solvent solubility provided the evidence to support the argument that the deposition problem was not the same as the precipitation problem. In other words, the deposition does not have the same dependence on the solvent solubility as the precipitation does. This information on the solvent effect can aid the industry to avoid the operation condition that produces the maximum amount of asphaltene deposition when developing asphaltene management strategies during crude oil recovery.

**3.7. Assessment of Asphaltene Inhibitor (AI).** The assessment of the AI used in this study was performed to illustrate and help understand how the QCM-D technique could be used to screen for inhibitor performance using the deposition method. From an earlier extensive screening study using several commercially available AIs for this particular oil, the inhibitor chosen for this study was found to be more promising. Using the developed testing metrics, the effect of this commercial AI on asphaltene deposition was tested under different conditions, as shown in Figure 15.

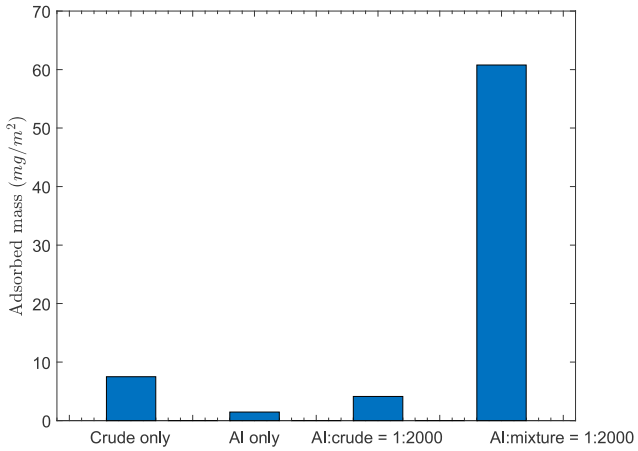


**Figure 15.** Measurement of the adsorbed mass under different conditions. The solvent mixture is composed of 80 vol% of heptane and 20 vol% of toluene for all cases. Crude only, dilution ratio of crude oil to heptane/toluene mixture is 1:20; AI only, mixing ratio of asphaltene inhibitor to heptane/toluene mixture is 1:2000 (i.e., 500 ppm); AI:crude = 1:2000, dilution ratio of crude oil to heptane/toluene mixture is 1:20 and mixing ratio of asphaltene inhibitor to crude oil is 1:2000; AI:mixture = 1:2000, dilution ratio of crude oil to heptane/toluene mixture is 1:20 and mixing ratio of asphaltene inhibitor to the heptane/toluene mixture is 1:2000.

In the case of no AI addition (i.e., crude only), the deposited mass is around 8 mg/m$^2$ after 2 h adsorption, which is above the Langmuir monolayer adsorption regime and implies the existence of multilayer buildup. With the addition of asphaltene inhibitors (i.e., AI:crude = 1:2000), it was observed that the amount deposited showed a significant decrease to around 4 mg/m$^2$, which corresponds to the monolayer regime. In order to explore the effect of the inhibitor concentration, the amount of the added AI was further increased (i.e., AI:mixture = 1:2000) at the same dilution ratio of crude oil to heptane/toluene solvent mixture as the previous case. The deposition was found to dramatically increase instead of showing further decrease. This could be caused by the formation of aggregates composed of inhibitor and asphaltene molecules upon the increase of AI concentration, as reported earlier.[73] The composition of the commercial inhibitor is unknown, and it is soluble in toluene. To exclude the possibility of AI molecules' self-aggregations, only AI was mixed with the solvent mixture at the ratio of 1:2000. We could observe a slight adsorption of the AI molecules, indicating that the commercial inhibitor probably interacts with the solid surface and leaves less space for asphaltene molecules to deposit. On the other hand, as the adsorbed mass is less than the monolayer coverage, we could infer that, at this concentration, the AI molecules did not interact with each other and only partially covered the solid surface. It could therefore be concluded from the above experiments that, with the addition of a small amount of AI, the asphaltene deposition was hindered and reduced; adding a large quantity of AI into the sample does not improve the effects but rather significantly increases the deposition. This is in line with the industry's expectations, as employing additives at low concentrations to


https://dx.doi.org/10.1021/acs.energyfuels.0c00663
Energy Fuels XXXX, XXX, XXX−XXX

improve the production efficiency and minimize the production cost is highly desired.

As solvent solubility can greatly affect asphaltene deposition, in order to investigate the performance of the AI at different solubilities, crude sample was mixed with a small amount of inhibitor solution and heptane/toluene solvent mixtures with different heptane percentages. In diluted samples (see Figure 16), the AI was found to reduce the adsorbed mass by at least

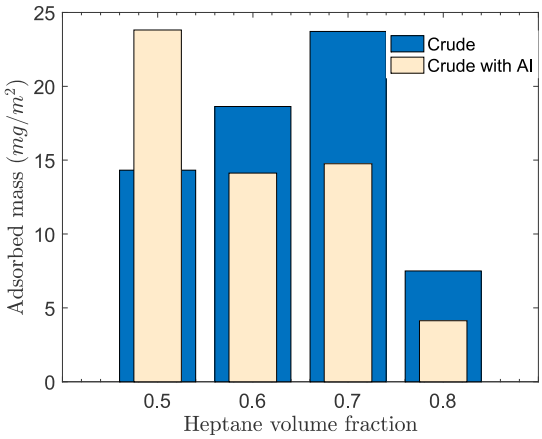


**Figure 16.** Adsorbed mass for crude oil in solvent mixture with different heptane/toluene ratios. The dilution ratio of oil to solvent mixture is 1:20, and the mixing ratio of AI to crude oil is 1:2000.

25% at higher heptane percentage, even though there is less asphaltene deposition at the solubility with the 80 vol% heptane in the solvent mixture. To the contrary, at the solubility with 50 vol% heptane and 50 vol% toluene, the inhibitor does not show any positive effect but the deposited amount increases. In a concentrated sample (see Figure 17),

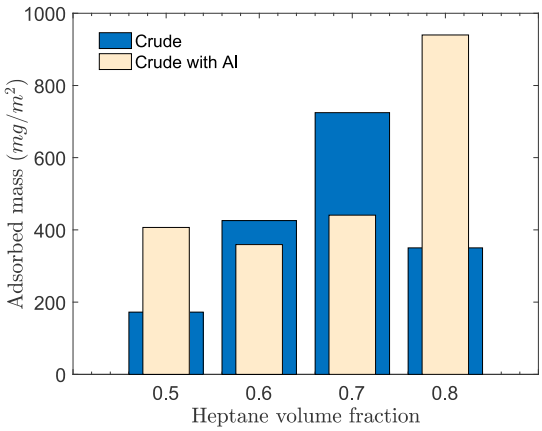


**Figure 17.** Adsorbed mass for crude oil in solvent mixture with different heptane/toluene ratios. The dilution ratio of oil to solvent mixture is 1:1, and the mixing ratio of AI to crude oil is 1:2000.

the AI gives promising performance only near the precipitation onset point, i.e., the solubility with 60 and 70 vol% heptane content. At the solubility with 50 and 80 vol% heptane fractions, the adsorbed mass with inhibitors exhibits a significant increase compared to the case with no addition of AI. One possible explanation for such a wide distribution of AI performance could be that the change in the solubility could result in the restructuring or reorientation of the AI molecules, which eventually alters the availability of their surface-active groups and their interaction with asphaltene molecules. Nevertheless, in both diluted and concentrated samples, the inhibitor proved to be able to reduce the maximum deposition amount at the solubility with 70 vol% heptane fraction, which happened to be the condition at which the largest amount of deposition was generated, as found from the previous experiments.

Asphaltene inhibitors are generally a mixture of subcomponents providing different functionalities. The results of this work are limited to the one inhibitor tested, but the experimental approach developed here could be used for screening other inhibitors in future studies.

## 4. CONCLUSIONS

The kinetics of asphaltene adsorption from crude oil onto stainless-steel surfaces at different mixing ratios with toluene are reported in this study. The size of the adsorbed particles from the initially diffusion-controlled adsorption was estimated and found to increase with the asphaltene concentration, except in the highly concentrated solutions (mixing ratio of crude oil to toluene of 4:1). The adsorption isotherm exhibited multiple regimes, which indicates a transition from monolayer to multilayer adsorption. The repetitive features presented in the initial adsorption kinetics and the $D-f$ ratios at different mixing ratios suggest a two-step deposition mechanism, where the first layer of asphaltene is adsorbed through the $\pi$-interaction of the polyaromatic hydrocarbons with the solid surface, followed by the subsequent layers of adsorbed molecules/aggregates interacting with the previously adsorbed molecules through alkyl chains. A numerical analysis of the experimental data using the two-step deposition model was performed, and the optimized adsorption parameters proved to be quite close to those values obtained for some rock types in earlier adsorption studies.[16]

The effect of solvent solubility on asphaltene deposition was also investigated by adding heptane into the solvent mixture at dilution ratios of 1:20 and 1:1. The adsorbed mass was found to first increase and then decrease with the heptane content at both dilution ratios, and it seems that the maximum deposition was reached at the solubility with a heptane/toluene ratio of 70:30. The correlation between heptane content and the deposition amount was found to be quite different from the conditions for asphaltene precipitation onset, which opens up the need to further investigate the structure of the precipitated asphaltenes and how they interact with the previously adsorbed molecules on the solid surfaces, with a potential impact on the wettability alteration of reservoir rocks and production facilities and asphaltene management in upstream production.

The impact of adding a commercial asphaltene inhibitor into crude oil sample solution was investigated under different conditions, and it was found that adding a small amount of AI could significantly reduce the deposited mass, but a large amount would have the reverse effects. The solubility could also affect the performance of the AI, and the AI exhibited a better performance near the onset point of precipitation in both dilute and concentrated sample. Nonetheless, since only a limited range of heptane/toluene ratios was tested, the postulation needs further experiments at other ratios to confirm how the deposited films vary.


https://dx.doi.org/10.1021/acs.energyfuels.0c00663
Energy Fuels XXXX, XXX, XXX−XXX

## AUTHOR INFORMATION


### Corresponding Author

**Fang Liu** − *Energy Institute, City University of New York, New York, New York 10031, United States; Department of Chemical Engineering, City College of New York, New York, New York 10031, United States;* orcid.org/0000-0001-7382-6215; Email: fangliuche@gmail.com

### Authors

**Scott Hickman** − *ExxonMobil Upstream Research Company, Spring, Texas 77389, United States*

**Tabish Maqbool** − *ExxonMobil Upstream Research Company, Spring, Texas 77389, United States*

⊥**Vincent Pauchard** − *SINTEF Industry, 7034 Trondheim, Norway;* orcid.org/0000-0003-1027-4526

**Sanjoy Banerjee** − *Energy Institute, City University of New York, New York, New York 10031, United States; Department of Chemical Engineering, City College of New York, New York, New York 10031, United States*

Complete contact information is available at: https://pubs.acs.org/10.1021/acs.energyfuels.0c00663


### Notes

The authors declare no competing financial interest.

⊥V.P. is a Consultant for SINTEF Industry, Norway, and City College of New York.

## ACKNOWLEDGMENTS

The authors thank Dr. Brendon Keinath, Dr. Todd Lagus, Dr. Aditya Jaishankar, Dr. Marykathryn Lee, Prof. Jeff Morris, and Prof. Charles Maldarelli for valuable technical discussions. The authors also thank Becky Whitt for help with measuring viscosity and density of samples and Todd Mayer, Jennifer Benton, and Rosario Jara for help on the QCM-D experiments. This work is supported by the National Science Foundation under Award Number 1743794.

## REFERENCES


(1) Buckley, J. S. Wetting Alteration of Solid Surfaces by Crude Oils and Their Asphaltenes. *Rev. Inst. Fr. Pet.* **1998**, *53*, 303−312.

(2) Akbarzadeh, K.; Hammami, A.; Kharrat, A.; Zhang, D.; Allenson, S.; Creek, J.; Kabir, S.; Jamaluddin, A. J.; Marshall, A. G.; Rodgers, R.; Mullins, O. C.; Solbakken, T. Asphaltenes — Problematic but Rich in Potential. *Oilfield Rev.* **2007**, *19*, 22−43.

(3) Creek, J. L. Freedom of action in the state of asphaltenes: Escape from conventional wisdom. *Energy Fuels* **2005**, *19*, 1212−1224.

(4) Jamaluddin, A. K. M.; Creek, J.; Kabir, C. S.; McFadden, J. D.; Cruz, D. D.; Manakalathil, J.; Joshi, N.; Ross, B. Laboratory Techniques to Measure Thermodynamic Asphaltene Instability. *J. Can. Pet. Technol.* **2002**, *41*, PETSOC-02-07-04.

(5) Burke, N. E.; Hobbs, R. E.; Kashou, S. F. Measurement and Modeling of Asphaltene Precipitation (includes associated paper 23831). *JPT, J. Pet. Technol.* **1990**, *42*, 1440−1446.

(6) Carrier, H.; Plantier, F.; Daridon, J.-L.; Lagourette, B.; Lu, Z. Acoustic method for measuring asphaltene flocculation in crude oils. *J. Pet. Sci. Eng.* **2000**, *27*, 111−117.

(7) Maqbool, T.; Balgoa, A. T.; Fogler, H. S. Revisiting Asphaltene Precipitation from Crude Oils: A Case of Neglected Kinetic Effects. *Energy Fuels* **2009**, *23*, 3681−3686.

(8) Kraiwattanawong, K.; et al. Thermodynamic solubility models to predict asphaltene instability in live crude oils. *Energy Fuels* **2007**, *21*, 1248−1255.

(9) Goual, L.; Sedghi, M.; Wang, X.; Zhu, Z. Asphaltene Aggregation and Impact of Alkylphenols. *Langmuir* **2014**, *30*, 5394−5403.

(10) Fossen, M.; Sjöblom, J.; Kallevik, H.; Jakobsson, J. A New Procedure for Direct Precipitation and Fractionation of Asphaltenes from Crude Oil. *J. Dispersion Sci. Technol.* **2007**, *28*, 193−197.

(11) Hammami, A.; Ratulowski, J. Precipitation and Deposition of Asphaltenes in Production Systems: A Flow Assurance Overview. In *Asphaltenes, Heavy Oils, and Petroleomics*; Mullins, O. C., Sheu, E. Y., Hammami, A., Marshall, A. G., Eds.; Springer: New York; pp 617−660.

(12) Hoepfner, M. P.; Limsakoune, V.; Chuenmeechao, V.; Maqbool, T.; Fogler, H. S. A Fundamental Study of Asphaltene Deposition. *Energy Fuels* **2013**, *27*, 725−735.

(13) Dudášová, D.; Simon, S.; Hemmingsen, P. V.; Sjöblom, J. Study of asphaltenes adsorption onto different minerals and clays. Colloids Surfaces A Physicochem. *Colloids Surf., A* **2008**, *317*, 1−9.

(14) Acevedo, S.; et al. Importance of asphaltene aggregation in solution in determining the adsorption of this sample on mineral surfaces. Colloids Surfaces A Physicochem. *Colloids Surf., A* **2000**, *166*, 145−152.

(15) Mugele, F.; Siretanu, I.; Kumar, N.; Bera, B.; Wang, L.; de Ruiter, R.; Maestro, A.; Duits, M.; van den Ende, D.; Collins, I. Insights From Ion Adsorption and Contact-Angle Alteration at Mineral Surfaces for Low-Salinity Waterflooding. *SPE J.* **2016**, *21*, 1204−1213.

(16) Mendoza de la Cruz, J. L.; et al. Study of monolayer to multilayer adsorption of asphaltenes on reservoir rock minerals. *Colloids Surf., A* **2009**, *340*, 149−154.

(17) Buckley, J. S.; Bousseau, C.; Liu, Y. Wetting Alteration by Brine and Crude Oil: From Contact Angles to Cores. *SPE J.* **1996**, *1*, 341−350.

(18) Crocker, M. E.; Marchin, L. M. Wettability and Adsorption Characteristics of Crude-Oil Asphaltene and Polar Fractions. *JPT, J. Pet. Technol.* **1988**, *40*, 470−474.

(19) Acevedo, S.; Ranaudo, M. A.; García, C.; Castillo, J.; Fernández, A. Adsorption of Asphaltenes at the Toluene−Silica Interface: A Kinetic Study. *Energy Fuels* **2003**, *17*, 257−261.

(20) Farooq, U.; Sjöblom, J.; Øye, G. Desorption of Asphaltenes from Silica-Coated Quartz Crystal Surfaces in Low Saline Aqueous Solutions. *J. Dispersion Sci. Technol.* **2011**, *32*, 1388−1395.

(21) Marczewski, A. W.; Szymula, M. Adsorption of asphaltenes from toluene on quartz and silica-rich soils. *Ann. Univ. Marie Curie-Sklodowska Lublin-Polonia* **2003**, *58*, 69−79.

(22) Smol, M.; Włodarczyk-Makuła, M.; Włóka, D. Adsorption of Polycyclic Aromatic Hydrocarbons (PAHS) from Aqueous Solutions on Different Sorbents. *Civ. Environ. Eng. Reports* **2014**, *13*, 87−96.

(23) Natarajan, A.; et al. Understanding Mechanisms of Asphaltene Adsorption from Organic Solvent on Mica. *Langmuir* **2014**, *30*, 9370−9377.

(24) Zhang, R.; Qin, N.; Peng, L.; Tang, K.; Ye, Z. Wettability alteration by trimeric cationic surfactant at water-wet/oil-wet mica mineral surfaces. *Appl. Surf. Sci.* **2012**, *258*, 7943−7949.

(25) Liu, L.; Buckley, J. S. Alteration of wetting of mica surfaces. *J. Pet. Sci. Eng.* **1999**, *24*, 75−83.

(26) Vuillaume, K.; Giasson, S. Interactions between Mica Surfaces across Crude Oil and Asphaltene Solutions. *J. Phys. Chem. C* **2009**, *113*, 3660−3665.

(27) Syunyaev, R. Z.; Balabin, R. M.; Akhatov, I. S.; Safieva, J. O. Adsorption of Petroleum Asphaltenes onto Reservoir Rock Sands Studied by Near-Infrared (NIR) Spectroscopy. *Energy Fuels* **2009**, *23*, 1230−1236.

(28) Marczewski, A. W.; Szymula, M. Adsorption of asphaltenes from toluene on mineral surface. *Colloids Surf., A* **2002**, *208*, 259−266.

(29) Szymula, M.; Marczewski, A. W. Adsorption of asphaltenes from toluene on typical soils of Lublin region. *Appl. Surf. Sci.* **2002**, *196*, 301−311.

(30) Clementz, D. M. Interaction of Petroleum Heavy Ends with Montmorillonite. *Clays Clay Miner.* **1976**, *24*, 312−319.

(31) Alboudwarej, H.; Pole, D.; Svrcek, W. Y.; Yarranton, H. W. Adsorption of Asphaltenes on Metals. *Ind. Eng. Chem. Res.* **2005**, *44*, 5585−5592.

(32) Xie, K.; Karan, K. Kinetics and Thermodynamics of Asphaltene Adsorption on Metal Surfaces: A Preliminary Study. *Energy Fuels* **2005**, *19*, 1252−1260.

(33) Rudrake, A.; Karan, K.; Horton, J. H. A combined QCM and XPS investigation of asphaltene adsorption on metal surfaces. *J. Colloid Interface Sci.* **2009**, *332*, 22−31.

(34) Ekholm, P.; et al. A Quartz Crystal Microbalance Study of the Adsorption of Asphaltenes and Resins onto a Hydrophilic Surface. *J. Colloid Interface Sci.* **2002**, *247*, 342−350.

(35) Zahabi, A.; Gray, M. R.; Dabros, T. Kinetics and Properties of Asphaltene Adsorption on Surfaces. *Energy Fuels* **2012**, *26*, 1009−1018.

(36) Ortega Rodriguez, A.; Cruz, S. A.; Garcia-Cruz, I.; Lira-Galeana, C. Study of the adhesion force of asphaltene aggregates to metallic surfaces of Fe and Al. *Energy Fuels* **2016**, *30*, 3596−3604.

(37) Balabin, R. M.; et al. Asphaltene Adsorption onto an Iron Surface: Combined Near-Infrared (NIR), Raman, and AFM Study of the Kinetics, Thermodynamics, and Layer Structure. *Energy Fuels* **2011**, *25*, 189−196.

(38) Abdallah, W. A.; Taylor, S. D. Surface characterization of adsorbed asphaltene on a stainless steel surface. *Nucl. Instrum. Methods Phys. Res., Sect. B* **2007**, *258*, 213−217.

(39) Dudášová, D.; Silset, A.; Sjöblom, J. Quartz Crystal Microbalance Monitoring of Asphaltene Adsorption/Deposition. *J. Dispersion Sci. Technol.* **2008**, *29*, 139−146.

(40) Collins, S. H.; Melrose, J. C. Adsorption of Asphaltenes and Water on Reservoir Rock Minerals. *SPE Oilfield Geothermal Chem. Symp.* **1983**, *8*, 11800-MS.

(41) Dubey, S. T.; Waxman, M. H. Asphaltene Adsorption and Desorption From Mineral Surfaces. *SPE Reservoir Eng.* **1991**, *6*, 389−395.

(42) Tavakkoli, M.; Panuganti, S. R.; Taghikhani, V.; Pishvaie, M. R.; Chapman, W. G. Asphaltene Deposition in Different Depositing Environments: Part 2. Real Oil. *Energy Fuels* **2014**, *28*, 3594−3603.

(43) Vargas, F. M.; et al. Development of a General Method for Modeling Asphaltene Stability. *Energy Fuels* **2009**, *23*, 1147−1154.

(44) Tavakkoli, M.; Panuganti, S. R.; Taghikhani, V.; Pishvaie, M. R.; Chapman, W. G. Precipitated Asphaltene Amount at High-Pressure and High-Temperature Conditions. *Energy Fuels* **2014**, *28*, 1596−1610.

(45) Hashmi, S. M.; Loewenberg, M.; Firoozabadi, A. Colloidal asphaltene deposition in laminar pipe flow: Flow rate and parametric effects. *Phys. Fluids* **2015**, *27*, 083302.

(46) Melendez-Alvarez, A. A.; et al. On the evaluation of the performance of asphaltene dispersants. *Fuel* **2016**, *179*, 210−220.

(47) Lin, Y.-J.; He, P.; Tavakkoli, M.; Mathew, N. T.; Fatt, Y. Y.; Chai, J. C.; Goharzadeh, A.; Vargas, F. M.; Biswal, S. L. Characterizing Asphaltene Deposition in the Presence of Chemical Dispersants in Porous Media Micromodels. *Energy Fuels* **2017**, *31*, 11660−11668.

(48) Lin, Y.-J.; et al. Examining Asphaltene Solubility on Deposition in Model Porous Media. *Langmuir* **2016**, *32*, 8729−8734.

(49) Abudu, A.; Goual, L. Adsorption of Crude Oil on Surfaces Using Quartz Crystal Microbalance with Dissipation (QCM-D) under Flow Conditions. *Energy Fuels* **2009**, *23*, 1237−1248.

(50) Campen, S.; Moorhouse, S. J.; Wong, J. S. S. Mechanism of an asphaltene inhibitor in different depositing environments: Influence of colloid stability. *J. Pet. Sci. Eng.* **2020**, *184*, 106502.

(51) Sauerbrey, G. Verwendung von Schwingquarzen zur Wägung dünner Schichten und zur Mikrowägung. *Eur. Phys. J. A* **1959**, *155*, 206−222.

(52) Rodahl, M.; Kasemo, B. On The Measurement Of Thin Liquid Overlayers With The Quartz-crystal Microbalance *Proceedings of the International Solid-State Sensors and Actuators Conference - TRANSDUCERS '95*; IEEE, 1995; Vol. *2*, pp 743−746.

(53) Kanazawa, K. K.; Gordon, J. G. Frequency of a quartz microbalance in contact with liquid. *Anal. Chem.* **1985**, *57*, 1770−1771.

(54) Sztukowski, D. M.; Jafari, M.; Alboudwarej, H.; Yarranton, H. W. Asphaltene self-association and water-in-hydrocarbon emulsions. *J. Colloid Interface Sci.* **2003**, *265*, 179−186.

(55) Goual, L.; Horváth-Szabó, G.; Masliyah, J. H.; Xu, Z. Adsorption of Bituminous Components at Oil/Water Interfaces Investigated by Quartz Crystal Microbalance: Implications to the Stability of Water-in-Oil Emulsions. *Langmuir* **2005**, *21*, 8278−8289.

(56) Liu, F.; et al. Mixture Effect on the Dilatation Rheology of Asphaltenes-Laden Interfaces. *Langmuir* **2017**, *33*, 1927−1942.

(57) Ward, A. F. H.; Tordai, L. Time-Dependence of Boundary Tensions of Solutions I. The Role of Diffusion in Time-Effects. *J. Chem. Phys.* **1946**, *14*, 453.

(58) Seifried, C. M.; Crawshaw, J.; Boek, E. S. Kinetics of Asphaltene Aggregation in Crude Oil Studied by Confocal Laser-Scanning Microscopy. *Energy Fuels* **2013**, *27*, 1865−1872.

(59) Mullins, O. C. The Asphaltenes. *Annu. Rev. Anal. Chem.* **2011**, *4*, 393−418.

(60) Mullins, O. C.; et al. The Colloidal Structure of Crude Oil and the Structure of Oil Reservoirs. *Energy Fuels* **2007**, *21*, 2785−2794.

(61) Mullins, O. C.; Pomerantz, A. E.; Andrews, A. B.; Zuo, J. Y. Asphaltenes Explained for the Nonchemist. *Petrophysics* **2015**, *56*, 266−275.

(62) Campen, S.; Di Mare, L.; Smith, B.; Wong, J. S. S. Determining the Kinetics of Asphaltene Adsorption from Toluene: A New Reaction-Diffusion Model. *Energy Fuels* **2017**, *31*, 9101−9116.

(63) Campen, S.; Smith, B.; Wong, J. Deposition of Asphaltene from Destabilized Dispersions in Heptane-Toluene. *Energy Fuels* **2018**, *32*, 9159−9171.

(64) Zhu, B.; Gu, T. Reverse hemimicelle formation of 1-decanol from heptane at the solution/graphite interface. *Colloids Surf.* **1990**, *46*, 339−345.

(65) Keiluweit, M.; Kleber, M. Molecular-level interactions in soils and sediments: The role of aromatic $\pi$-systems. *Environ. Sci. Technol.* **2009**, *43*, 3421−3429.

(66) Rane, J. P.; Pauchard, V.; Couzis, A.; Banerjee, S. Interfacial rheology of asphaltenes at oil-water interfaces and interpretation of the equation of state. *Langmuir* **2013**, *29*, 4750−4759.

(67) Zarkar, S.; Pauchard, V.; Farooq, U.; Couzis, A.; Banerjee, S. Interfacial Properties of Asphaltenes at Toluene - Water Interfaces. *Langmuir* **2015**, *31*, 4878−4886.

(68) Rane, J. P.; et al. Applicability of the Langmuir Equation of State for Asphaltene Adsorption at the Oil–Water Interface: Coal-Derived, Petroleum, and Synthetic Asphaltenes. *Energy Fuels* **2015**, *29*, 3584−3590.

(69) Pauchard, V.; Roy, T. Blockage of coalescence of water droplets in asphaltenes solutions: A jamming perspective. *Colloids Surf., A* **2014**, *443*, 410−417.

(70) Mullins, O. C.; et al. Asphaltene Nanoscience and Reservoir Fluid Gradients, Tar Mat Formation and the Oil-Water Interface. *SPE Annual Technical Conference and Exhibition*; Society of Petroleum Engineers, 2013. .

(71) Pauchard, V.; Rane, J. P.; Zarkar, S.; Couzis, A.; Banerjee, S. Long-Term Adsorption Kinetics of Asphaltenes at the Oil−Water Interface: A Random Sequential Adsorption Perspective. *Langmuir* **2014**, *30*, 8381−8390.

(72) Mullins, O. C. The Modified Yen Model. *Energy Fuels* **2010**, *24*, 2179−2207.

(73) Balestrin, L. B. d. S.; Francisco, R. D.; Bertran, C. A.; Cardoso, M. B.; Loh, W. Direct Assessment of Inhibitor and Solvent Effects on the Deposition Mechanism of Asphaltenes in a Brazilian Crude Oil. *Energy Fuels* **2019**, *33*, 4748−4757.

(74) Hannisdal, A.; Ese, M.-H.; Hemmingsen, P. V.; Sjöblom, J. Particle-stabilized emulsions: Effect of heavy crude oil components pre-adsorbed onto stabilizing solids. *Colloids Surf., A* **2006**, *276*, 45−58.


https://dx.doi.org/10.1021/acs.energyfuels.0c00663
Energy Fuels XXXX, XXX, XXX−XXX

(75) Maqbool, T.; Raha, S.; Hoepfner, M. P.; Fogler, H. S. Modeling the Aggregation of Asphaltene Nanoaggregates in Crude Oil–Precipitant Systems. *Energy Fuels* **2011**, *25*, 1585–1596.

(76) Fossen, M.; Kallevik, H.; Knudsen, K. D.; Sjöblom, J. Asphaltenes Precipitated by a Two-Step Precipitation Procedure. 2. Physical and Chemical Characteristics. *Energy Fuels* **2011**, *25*, 3552–3567.

(77) Spiecker, P. M.; Gawrys, K. L.; Kilpatrick, P. K. Aggregation and solubility behavior of asphaltenes and their subfractions. *J. Colloid Interface Sci.* **2003**, *267*, 178–193.

(78) Elkhatib, O.; Chaisoontornyotin, W.; Gesho, M.; Goual, L. Nanoscale investigation of asphaltene deposition under capillary flow conditions. *Energy Fuels* **2020**, *34*, 5148–5158.

(79) Groenzin, H.; et al. Molecular Size of Asphaltene Solubility Fractions. *Energy Fuels* **2003**, *17*, 498–503.

(80) Castillo, J.; et al. Study of the aggregation and adsorption of asphaltene sub-fractions A1 and A2 by white light interferometry: Importance of A1 sub-fraction in the aggregation process. *Colloids Surf., A* **2013**, *427*, 41–46.

(81) Fenistein, D.; et al. Viscosimetric and Neutron Scattering Study of Asphaltene Aggregates in Mixed Toluene/Heptane Solvents. *Langmuir* **1998**, *14*, 1013–1020.

(82) Spiecker, P. M.; Kilpatrick, P. K. Interfacial Rheology of Petroleum Asphaltenes at the Oil–Water Interface. *Langmuir* **2004**, *20*, 4022–4032.

(83) Jestin, J.; Simon, S.; Zupancic, L.; Barré, L. A Small Angle Neutron Scattering Study of the Adsorbed Asphaltene Layer in Water-in-Hydrocarbon Emulsions: Structural Description Related to Stability. *Langmuir* **2007**, *23*, 10471–10478.



https://dx.doi.org/10.1021/acs.energyfuels.0c00663
*Energy Fuels* XXXX, XXX, XXX–XXX